Binding of Nitric Oxide to First-Transition-Row Metal Cations: An *ab Initio* Study

Julie L.C. Thomas,[†] Charles W. Bauschlicher, Jr.,*[,‡] and Michael B. Hall*[,†]

Texas A&M University, Department of Chemistry, College Station, Texas 77843-3255, and National Aeronautics and Space Adminstration Ames Research Center, Moffett Field, California 94035-1000

Received: May 2, 1997[⊗]

Equilibrium geometries and binding energies have been determined for several states of the transition metal nitrosyl cations, $M(NO)^+$, for the first-transition-row metals, scandium through copper, (M = Sc−Cu). The geometries were optimized using density functional theory (DFT) with a hybrid functional (B3LYP). Our calculations predict that the ground states for $Sc(NO)^+$, $Ti(NO)^+$, and $V(NO)^+$ have side-on geometries with the N and O approximately equidistant from the metal center. In these structures, N and O both form covalent bonds with the metal center. The ground states of $M(NO)^+$ for chromium through nickel are linearly bound at the nitrogen and Cr^+-Co^+ form bonds that are primarily electrostatic and dative in nature. Ground-state $Ni(NO)^+$ is more strongly bound than the other linear $M(NO)^+$ complexes, due to a larger contribution from NO to metal charge transfer in the bonding. Ground-state $Cu(NO)^+$ has a bent structure with a one-electron bond between the Cu and N. All the ground-state electronic configurations are dominated by d^{n+1} occupations of the metals. Binding energies were calculated with both DFT and the coupled cluster approximation with single and double excitations and perturbational estimate of the triple excitations (CCSD(T)) and corrected for zero-point energy. The binding energies for the ground-state complexes calculated with respect to the ground states of the metal ions at the CCSD(T) level increase from Sc to Ti, decrease to Mn, then increase again to nickel, decreasing again to copper. We found that the DFT binding energies for the ground-state complexes in this system were larger than the CCSD(T) values by as little as 3 kcal/mol for $Sc(NO)^+$ and $Co(NO)^+$ and as much as 17 kcal/mol for $Mn(NO)^+$, except for $Ti(NO)^+$ and $Ni(NO)^+$, where the DFT binding energies are 6.3 and 7.4 kcal/mol smaller than the CCSD(T) value, respectively. The weaker bond strengths in the middle of the transition row can be attributed to the dominance of electrostatic contributions in the bonding of these $M(NO)^+$ complexes. Excluding Cu, the M−NO bonds are stronger at either end of the row where the contribution from covalent bonding is larger.

1. Introduction

The reactions of nitric oxide with transition metals are of interest in several areas, including biochemical systems, atmospheric chemistry, and surface chemistry. Nitric oxide acts as a potent bioregulator in several heme-containing enzymatic cycles.[1] The binding of nitric oxide to heme iron centers in metalloproteins is often a crucial protective step in the enzymes' reactions to combat toxins in the body. The chemistry of NO is an environmental concern in both the upper and lower atmosphere. Nitric oxide undergoes primarily charge transfer reactions in the ionosphere[2] where it contributes to ozone depletion. In the troposphere, NO is implicated in photodissociative production of smog, which also contains a number of transition metals, e.g., titanium, lead, zinc, iron, vanadium, manganese, and nickel, in highly polluted areas.[3] As nitric oxide is also a byproduct in the combustion of fossil fuels in automobiles, reactions involving NO on metal surfaces are important in the development of efficient catalysts for use in catalytic converters.[4]

The investigation of transition metal ion-molecule reactivity has seen tremendous growth in the past decade. In the course of the accumulation of the large body of data that is now available, there has been significant interplay between theory and experiment as accurate descriptions of the characteristics of these systems have been established. This synergistic effort between theory and experiment continues to be characteristic of the field of ion-molecule chemistry. Theoretical studies have successfully reproduced experimental results and disagreement between theory and experiment often instigates more accurate experimental studies as well as more accurate computational studies. This improved body of experimental and theoretical data can often explain previously anomalous results.

Many studies have been conducted on small molecules interacting with bare metal cations,[5] e.g., CH_4, CH_2, C_2H_4, CO, O_2, and H_2. NO, however, has been largely ignored. Studies by Cassady and Freiser[6] report bond energies for iron, cobalt, and nickel:

$$34 \pm 2 < D_0[Fe(NO)^+] < 58 \pm 2 \text{ kcal/mol},$$

$$37 \pm 2 < D_0[Co(NO)^+] < 52 \pm 2 \text{ kcal/mol, and}$$

$$D_0[Ni(NO)^+] = \sim 43 \text{ kcal/mol}$$

Khan et al.[7] studied the sequential bond energies of $Ni(CO)_x^+$, $Ni(N_2)_x^+$ ($x = 1-4$), and $Ni(NO)_x^+$ ($x = 1-3$). Results determined by collision-induced dissociation in a guided ion beam mass spectrometer show the bond dissociation energy for $Ni(NO)^+$ to be 54 ± 2 kcal/mol. This value is larger than that reported earlier.[6] Schwarz and co-workers[8] studied CuNO and $Cu(NO)^+$ with collisional activation and neutralization reionization mass spectrometry and suggested that the structure of the individual molecules was either a side-on geometry or two rapidly interconverting end-on geometries. Oriedo and Russell[9] examined the reactivity of NO with Fe^+ in Fourier transform ion cyclotron resonance mass spectrometry experiments and discovered that only excited states of Fe^+ react with NO. By removing the products of the reactions by mass selection, they successfully isolated beams of Fe^+ that contained only the

[†] Texas A&M University.
[‡] NASA Ames Research Center.
* Corresponding Authors. MBH, E-mail: hall@chemvx.chem.tamu.edu. CWB, E-mail: bauschli@pegasus.arc.nasa.gov.
[⊗] Abstract published in *Advance ACS Abstracts,* October 15, 1997.

S1089-5639(97)01493-X CCC: $14.00

unreactive ground state of Fe^+ $^6D(d^6s^1)$ and an unreactive excited state, the identity of which they proposed to be $^6S(d^5s^2)$. Several studies have examined the interaction of NO with the second- and third-transition-row metals, particularly the noble metals so important in catalysis,[10] but the first transition row remains largely uninvestigated.

Computational studies of the reactivity of NO with first-transition-row metal ions have been limited to $Cu(NO)^+$. Hrušák et al.[11] conducted studies of the isomers and excited states of $Cu(NO)^+$ and neutral CuNO, with CCSD(T). Benjelloun et al.[12] conducted similar studies with self-consistent field (SCF) and the configuration interaction (CI) methods. These two studies reported conflicting results. Hrušák et al. predicted a bent, $^2A'$ ground state, bound by 19.3 kcal/mol, while Benjelloun et al. predicted a linear $^2\Pi$ ground state bound by 37.52 kcal/mol. In the work of Benjelloun et al. the first excited state of $Cu(NO)^+$ is $^2A'$ and lies 19.8 kcal/mol above the ground state at the CI level. The neutral species NiNO has also been investigated,[13] as have the neutral and cationic systems of palladium and platinum,[14] but there are no studies of other first-transition-row metal cationic systems.

In this work we have undertaken an ab initio study of the equilibrium geometries and binding energies of NO with the metal cations of the first transition row, scandium to copper. We use density functional theory (DFT) to optimize the geometries and determine the binding energies of several states of these $M(NO)^+$ complexes. DFT has proven successful in determining equilibrium geometries in similar transition metal systems where an atom or cation interacts with small molecules.[15] The coupled-cluster approximation, which we also use to calculate the binding energies, represents one of the most accurate ab initio methods available at the present time. While it is possible to optimize geometries using this highly correlated method, DFT has the advantage of producing equilibrium geometries that are comparable in quality to those obtained with more highly correlated methods at a fraction of the computational cost. Having both the DFT and CCSD(T) binding energies will provide an opportunity to assess the accuracy of both methods in treating a system containing several challenging factors: a transition metal, excited-state reactants and products, and open-shell reactants and products.

2. Methods

2.1. Basis Sets. For the transition metals in this study we use three basis sets. The first two are based on those published by Wachters.[16] The first uses the primitive set (14s *9*p *5*d), contracted to [8s *4*p *3*d] (contraction 3). The d-space is contracted (311). Two additional p functions, one diffuse d function,[17] and three f polarization functions[18] are also added. The p functions are those optimized by Wachters, multiplied by 1.5. This basis set for the transition metals, denoted AW, has the final form (14s 11p 6d 3f)/[8s 6p 4d 1f]. The second basis set for the transition metals is denoted 6-311+G(2df) in GAUSSIAN94. This basis set is also based on the Wachters' primitives, but it uses the scaling factors of Raghavachari and Trucks.[19] This larger basis set has more flexible contractions of the s and p spaces, two additional p functions, a diffuse d function,[17] two uncontracted f functions, and one uncontracted g function.[20] The final form of the 6-311+G(2df) basis set is (15s 11p 6d 2f 1g)/[10s 7p 4d 2f 1g]. The third transition-metal basis set is derived from the primitive functions optimized by Partridge.[21] This basis set, denoted AANO (averaged atomic natural orbitals[22]), has the form (20s 15p 10d 6f 4g)/[7s 6p 4d 2f 1g] and is described in detail elsewhere.[18] For calculations on the ground states of $Sc(NO)^+$ and $Ti(NO)^+$, the 3s and 3p orbitals of Sc^+ and Ti^+ are of sufficient energy and radial extent to mix with the 2s orbitals of the NO. To correctly describe this mixing, in the AANO basis sets for Sc and Ti, the contractions of the 3s and 3p orbitals are altered to allow for more flexibility in these orbitals. For Sc and Ti the first 17s functions are contracted to 3 functions using the AANO orbitals while the four most diffuse s primitives are uncontracted. The first ten p functions are contracted to two functions, while the six most diffuse primitives are uncontracted. The four d AANOs are supplemented by uncontracting two d functions in the region of the 3p orbital, namely those with exponents of 1.342 621 and 0.561 524 for Sc and 1.689 268 9 and 0.715 670 6 for Ti. The unmodified three f and two g polarization sets are used. Thus the final Sc and Ti basis sets are of the form (21s 16p 9d 6f 4g)/[7s 8p 6d 3f 2g] and are denoted AANO3s3p.

Several basis sets were used throughout the course of the study for the main group atoms. The double-ζ plus polarization (DZP) set is derived from the primitive set optimized by van Duijneveldt[23] with a d polarization function added,[24] and the DZP was used for the geometry optimizations and the calculations of the DFT binding energies for the $M(NO)^+$ complexes. The form of this basis set is (9s 5p 1d)/[4s 3p 1d], in which the s-space is contracted (5211). Dunning's correlation-consistent polarized valence triple-ζ basis set (cc-pVTZ)[25] was used for the calculation of the CCSD(T) binding energies. The form of the cc-pVTZ basis set for C, N, and O is (10s 5p 2d 1f)/[4s 3p 2d 1f]. The 6-311+G(2df) basis set was also used for N and O in a DFT calculation. This basis set contains a significantly larger description of the N and O. A diffuse sp function, two d functions, and an f function are added to the 6-311G basis set[26] for N and O.

For the preliminary studies described below, 6-31G*[27] was used for all atoms in the DFT geometry optimization performed on $Na(NO)^+$ and cc-pVTZ was used for the CCSD(T) energy calculations. For the CCSD(T) calculations on $Na(NO)^+$ the 2s−2p space in Na was uncontracted to allow for flexibility in these orbitals. Two d functions were also added, with exponents of 3.0252 and 1.152 84. The f function is unmodified. The final form of the basis set is (16s 10p 4d 1f)/[6s 7p 4d 1f]. Dunning's correlation-consistent valence double-ζ basis set[25] was used for all atoms for the DFT geometry optimizations of H(NO) and $H(NO)^+$. The cc-pVTZ basis set was used for the CCSD(T) calculation of the binding energies. For ScCO, the AW/DZP was used for the DFT geometry optimizations and the AANO3s3p/cc-pVTZ was used for the CCSD(T) calculation of the binding energy.

2.2. Correlation Treatments. The hybrid[28] B3LYP [29−32] functional is used in all of the DFT calculations. While the B3LYP approach yields excellent geometries in general, it is known to have a bias for the d^{n+1} occupation over the d^ns^1. This can result in an incorrect order of molecular states. Futhermore, as it is usually implemented for open-shell systems, a spin-unrestricted DFT calculation can yield a solution contaminated by states of higher S^2 than the one desired. Since the S^2 value has proven useful in detecting problems for unrestricted Hartree−Fock (HF) wave functions, we compute S^2 values for the DFT orbitals assuming they correspond to a single determinental HF wave function. While clearly not rigorous, this approach may give some clue to the reliability of the DFT approach. Given that the S^2 values for some of the low-lying states for the molecules in the middle of the row (V−Co) can be very poor (see below), it is desirable that calibration calculations be performed using a spin-restricted-based approach. For these calibration calculations, we use the coupled-cluster singles and doubles approach,[33] including a perturbational estimate of the contribution of the triple excitations.[34] This method is commonly denoted CCSD(T). The implementation

we use is partially spin-restricted open-shell coupled-cluster theory. In this method, a high-spin-restricted Hartree-Fock reference wave function is used and certain restrictions in the amplitudes are introduced to calculate the linear portion of the wave function as a spin eigenfunction.[35]

2.3. Geometry Optimizations. The $M(NO)^+$ complexes were examined in three different geometries: linear, bent, and side-on. The equilibrium geometries are optimized at the DFT level for the orbital occupations associated with lowest molecular states of each spin and symmetry arising from the lowest atomic asymptotes for each metal cation reacting with NO. Frequency calculations were also performed at the DFT level to establish whether stationary points from the geometry optimization calculations were local minima or saddle points and to determine the zero-point energies.

2.4. Energetics. The DFT binding energies were computed in the AW/DZP basis set since DFT is less sensitive to basis set quality than CCSD(T). This aspect of DFT energetics has been discussed previously[15] and is confirmed for $M(NO)^+$ as we will show later. In the DFT treatment of the atomic ions, we use an occupation that corresponds to 100% ground state, i.e., we use the same occupation in the DFT approach as would be used in a Hartree-Fock calculation of the ground state. All solutions correspond to an integral number of 3d and 4s electrons. We use the occupation that corresponds to the true ion ground state regardless of the order of the states at the DFT level. Ricca and Bauschlicher[36] have proposed a method to correct for the bias in the DFT method that favors d^{n+1} states over $d^n s^1$ states. This bias would produce binding energies that are too large for systems where the binding in $M(NO)^+$ arises from the d^{n+1} occupation and the ground state of the free metal cation is $d^n s^1$. The corrected binding energies are obtained using the error in the atomic ion $d^n s^1 - d^{n+1}$ separation and the metal d populations in the molecule as a measure of the mixing of the atomic asymptotes in the molecular system. This correction was applied to the binding energies of the ground-state and certain low-lying $M(NO)^+$ complexes. DFT binding energies reported for other complexes and excited states of the $M(NO)^+$ complexes are not corrected. Binding energies for the ground states are also corrected for zero-point energy.

The CCSD(T) calculations were performed in the AW/cc-pVTZ and AANO/cc-pVTZ basis sets. Uncorrelated orbitals in the CCSD(T) calculations include the 1s-, 2s-, 2p-, 3s-, and 3p-like orbitals on the transition metals, except for calculations performed using the AANO basis set for complexes containing Sc and Ti, where the 3s and 3p electrons are also correlated. Uncorrelated orbitals for the main group and alkali metal atoms include the 1s-like orbitals on C, N, O, and Na. Binding energies for the AANO/cc-pVTZ basis are reported only for the ground and certain low-lying states of $M(NO)^+$. The AANO/cc-pVTZ binding energies are corrected for zero-point energy using the DFT vibrational frequencies. Relative energies are reported for most excited-state complexes at the DFT level in the AW/DZP basis set and at the CCSD(T) level in the AW/cc-pVTZ basis set. Complexes for which the CCSD(T) relative energetics are not reported are those for which the CCSD(T) energy could not be calculated due to significant multireference character in the wave function.

2.5. Preliminary Studies. To assess the ability of both DFT and CCSD(T) to successfully model different contributions to bonding in the $M(NO)^+$ complexes, we also looked at the NO molecule as well as three additional systems that would display single-component bonding with NO. $Na(NO)^+$ would be expected to display primarily electrostatic bonding arising from the attractive charge−dipole interaction. HNO, on the other hand, would display primarily covalent bonding, forming a single bond between the hydrogen and nitrogen and a double bond between N and O. HNO^+ serves as a model for systems containing a one-electron bond. ScCO is a well-characterized transition-metal system that displays traditional donor−acceptor or dative bonding. Comparison of these additional calculations to their experimental results and comparison between the CCSD(T) and DFT results may give us an indication of where discrepancies might occur in our calculations on the $M(NO)^+$ systems.

The DFT and CCSD(T) bond lengths for NO are consistent with each other at 1.157 and 1.156 Å, respectively, but slightly too long compared to the experimental value, 1.151 Å.[37] The bonding energies are more disparate, however. The experimental dissociation energy of NO is 151.1 kcal/mol.[37] The DFT value of $D_0 = 146.0$ kcal/mol for the DZP basis is 5 kcal/mol too small and the CCSD(T) value of $D_0 = 140.7$ kcal/mol for the cc-pVTZ basis is 10 kcal/mol too small. The ionization potential for NO at the DFT and CCSD(T) levels is also in error. The DFT IP is 9.71 eV, compared to the experimental value of 9.26 eV,[37] and the CCSD(T) value is 9.06 eV. Calculations of the dipole of NO showed that the DFT value is significantly too small at 0.0364 D, compared to the experimental value of 0.153 D.[37] The CCSD(T) value, 0.129 D, is much closer to the experimental value, but still slightly too small. Calculations performed with both methods would, therefore, underestimate the strength of a charge−dipole interaction, DFT more so than CCSD(T).

Results for HNO agree very well between DFT and CCSD(T). HNO has a bent geometry and a $^1A'$ ground state. The H-N bond distance is 1.078 Å and the N−O bond distance is 1.203 Å, compared to the experimental values of 1.063 Å and 1.212 Å.[38] The N−O bond is now a double bond because the electron in the π^* orbital of free NO is used to form a covalent bond with hydrogen and N rehybridizes from *sp* to sp^2. This change in bonding is evident from the longer N−O bond versus free NO. Results for the H-NO binding energy agree very well between the DFT and CCSD(T) methods, and both methods are in reasonable agreement with the experimental bond dissociation energy $D_0 = 48.6$ kcal/mol.[38] The DFT binding energy, corrected for zero-point energy, is $D_0 = 43.1$ kcal/mol and the CCSD(T) binding energy is $D_0 = 45.4$ kcal/mol.

HNO^+ has a bent geometry and a $^2A'$ ground state. The H-N bond distance is 1.088 Å and the N−O bond distance is 1.128 Å. In this case nitrogen does not rehybridize and instead the unpaired electron resides in an orbital formed from the NO π^* and H 1s orbitals, i.e., a one-electron bond is formed. In contrast to the N−O double bond in HNO, the N−O bond in HNO^+ is much closer to a triple bond. This increase in bond order can be seen in the short N−O bond distance in HNO^+. The DFT H^+-NO binding energy is 127.6 kcal/mol and the CCSD(T) binding energy is 128.0 kcal/mol. While there is no experimental data available, DFT and CCSD(T) are consistent in their description of a one-electron bond in a main group system.

In contrast to HNO and HNO^+, $Na(NO)^+$ has a linear $^2\Pi$ ground state. The Na−N bond distance is 2.423 Å and the N−O bond distance is 1.148 Å. The DFT binding energy is 1.31 kcal/mol; the CCSD(T) binding energy is 8.07 kcal/mol. Because of the error in the calculated dipole of NO described above, we would expect the CCSD(T) results to slightly underestimate the strength of a predominantly charge−dipole interaction, while the DFT results would err in the same direction, but more severely.

Neutral transition metal CO compounds exhibit primarily donor−acceptor binding. Using the modified coupled pair functional (MCPF) approach, Barnes and Bauschlicher[39] calculated the ground state of ScCO to be $^4\Sigma^-$, bound by $D_e =$

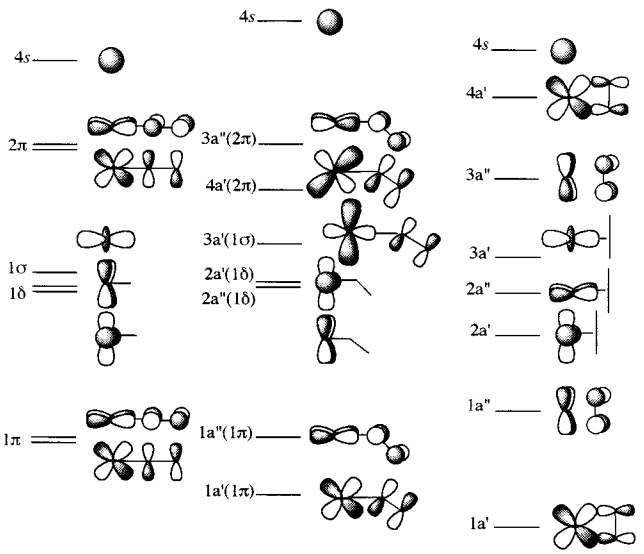

Figure 1. Evolution of the extended Hückel theory orbitals. The orbitals are shown corresponding to the qualitative energy levels for orbitals calculated at the EHT level for $Cr(NO)^+$ (linear), $Ni(NO)^+$ (bent), and $Sc(NO)^+$ (side-on). These qualitative orbitals are useful for describing how electrons would fill the orbitals in the $M(NO)^+$ complexes.

39.20 kcal/mol with respect to the $^4F(d^2s^1)$ state of Sc. Our results at the DFT level show ScCO bound by $D_e = 33.56$ kcal/mol in the AW/DZP basis set. In agreement with our DFT result, the CCSD(T) value for the binding energy of ScCO is $D_e = 33.31$ kcal/mol for the AANO3s3p/cc-pVTZ basis set. Both are 6 kcal/mol lower than the MCPF value. The CCSD(T) result strongly suggests that the MCPF value is too large.

From the results for NO, HNO, HNO^+, $Na(NO)^+$, and ScCO, we can see that the treatment of typical covalent, electrostatic, and dative bonds in both DFT and CCSD(T) is consistent between the two methods, and both should be able to describe the possible contributions to bonding in the $M(NO)^+$ complexes. Except for the weaker electrostatic contributions based on the magnitude of the NO dipole moment, we see no evidence that DFT will not work as well for the $M(NO)^+$ complexes as it has for many other transition metal systems.

2.6. Programs. The DFT calculations were performed with the GAUSSIAN94 suite of programs,[40] while the CCSD(T) calculations were performed with the MOLPRO96 program system.[41] Calculations were carried out the NASA Ames Research Center Computational Chemistry Branch IBM RISC System/6000 computers, the SGI Power Challenge machines at the Texas A&M University Supercomputer Center, the IBM-SP2 at the Cornell Theory Center, the SGI Power Challenge machine at the Texas A&M University Department of Chemistry, and SGI Power Indigo2 computers in the Hall research group at Texas A&M University.

3. Qualitative Considerations

There are three geometries possible for NO binding to a bare metal cation: linear, bent, and side-on. With extended Hückel theory[42] (EHT), we can establish qualitative bonding mechanisms. From EHT calculations performed on $Sc(NO)^+$, $Cr(NO)^+$, and $Ni(NO)^+$ we have constructed the qualitative molecular orbital diagram shown in Figure 1. In the linear geometry only the dπ orbitals are of the correct symmetry and energy to interact with the partially filled π^* orbital of NO. The interaction of the metal 3d and the NO π^* produces the following orbitals: two M−NO bonding orbitals, designated 1π; three nonbonding orbitals, 1σ and 1δ, in which the 1σ orbital is slightly destabilized compared to the 1δ orbitals; and two M−NO antibonding orbitals, 2π.

Upon bending of the $M(NO)^+$ molecule, the degenerate orbitals from the linear geometry split. The π-bonding orbitals form the 1a′(1π) and 1a″(1π) orbitals. The 1a′(1π) is lower in energy as bending increases the orbital overlap between the metal orbitals and the NO π^* orbital. Bending has a much smaller effect on the stability of the 1a″(1π) and 3a″(2π) orbitals as the overlap between the out-of-plane π-type orbitals is not significantly changed. The nonbonding orbitals also remain largely unchanged upon bending. The 4a′(2π) orbital mixes with the 4s orbital, which stabilizes the 4a′(2π) and destabilizes the 4s.

Side-on bonding produces a drastic change in the character of the orbitals of $M(NO)^+$. The 1a′ orbital is a σ-type bonding orbital formed from the in-plane, formerly dπ orbital, interacting with both the nitrogen and oxygen components of the in-plane π^* orbital of NO. The out-of-plane dπ orbital forms a π-type bond, 1a″, with the out-of-plane NO π^* orbital. The other metal d orbitals give rise to three nonbonding orbitals, 2a′, 2a″, and 3a′, that are directed at the nodes of the NO π^* orbitals.

For systems with the fewest electrons, we expect that side-on geometries would be preferred. The orbitals designated 1a′ and 1a″ in the side-on geometry are lower in energy than that of the π orbitals of the linear geometry or the 1a′(1π) and 1a″-(1π) orbitals of the bent geometry. For $Sc(NO)^+$ with three valence electrons, the side-on structure would appear to be favored as all the valence electrons are in covalent bonding orbitals. Covalent bonding is favored for the early metals because of the larger radial extent of the 3d orbitals. For $Ti(NO)^+$, the additional electron can add either to the bonding orbital or to one of the nonbonding δ-type orbitals. The latter option retains some of the atomic d−d exchange; however, the former is stabilized by additional covalent bonding with the N and O, so it is difficult to say which would be favored. For $V(NO)^+$ we would expect the additional electron to occupy a nonbonding orbital. Alternatively, the loss of d−d exchange energy for covalent bond formation might be sufficiently large that $V(NO)^+$ would have a high-spin configuration and a linear geometry. Both side-on and linear geometries will be evaluated for $V(NO)^+$. In the side-on geometry, $Cr(NO)^+$ would add an electron in the 3a′ dσ-type orbital which would increase the Cr^+−NO repulsion. A triplet state of $Cr(NO)^+$ could avoid this repulsive interaction by filling the 1a″ and 2a′ orbitals; however, the high exchange energy of Cr^+ makes it unlikely that a triplet state would be the ground state of $Cr(NO)^+$. $M(NO)^+$ complexes of the metal cations to the right of Cr^+ would add electrons to the even less favorable antibonding orbitals; thus, the $M(NO)^+$ complexes for M = Cr−Ni are expected to be linear.

For $Cu(NO)^+$ at the end of the first transition-row, the nonbonding d-manifold is filled and electrons must occupy the antibonding 2π orbitals. This unfavorable interaction, combined with the stability of the closed d^{10} shell, serves to localize the Cu^+ 3d orbitals and the NO π^* orbital. These localized orbitals present a different picture of the molecular orbitals than that shown in Figure 1. The 1π orbitals for linear $Cu(NO)^+$ would be predominantly Cu 3d and the 2π orbitals would be almost entirely NO π^*. For a linear geometry of $Cu(NO)^+$ we would expect almost entirely electrostatic bonding. The orbitals for bent $Cu(NO)^+$ would remain highly localized, but mixing between the in-plane NO π^* orbital and the 4s orbital of Cu^+ allows donation of electron density from the NO to metal center. This donation forms a one-electron σ-type interaction that introduces a dative component to the bond.

For the early metal cations, where the second ionization potential is low, we expect some contributions from the $M^{2+} + NO^-$ states. Since NO^- as a ligand is usually found bent in complexes, we might anticipate nonlinear structures for the early

metals. In the middle of the first row the second ionization potentials are much higher and we would expect contributions primarily from the ion−dipole interaction in $M^+ + NO$. $M(NO)^+$ complexes of the metals in the middle of the row would, therefore, be linear. For later metals we would also anticipate contributions from the charge transfer products, $M + NO^+$. This latter charge transfer contribution could be identified by shorter N−O bonds in the complexes, compared to free NO, since this charge transfer removes an electron from the antibonding NO π^* orbital.

Basic thermodynamic considerations can also provide some clues to the reaction of M^+ with NO. For a metal cation to cleave the N−O bond, the bond strength of the metal oxide or nitride cation, $M-O^+$ or $M-N^+$, must equal or exceed the binding energy of NO which is 150.71 ± 0.03 kcal/mol.[38] This situation only exists for Sc^+ and Ti^+, where the $M-O^+$ experimental binding energies are 164.6 ± 1.3 kcal/mol[43a,b] and 158.7 ± 1.6 kcal/mol,[43b] respectively. There might, therefore, exist low-lying equilibrium geometries for $Sc(NO)^+$ and $Ti(NO)^+$ that lie on the reaction pathway to the formation of $MO^+ + N$. Side-on geometries for the other metals, V^+-Cu^+, might also be observed, but we would not expect these to be as low in energy as those we expect for $Sc(NO)^+$ and $Ti(NO)^+$.

4. Results

We have optimized the geometries and calculated the binding energies of the lowest state of each spin and space symmetry arising from the d^ns^1 and d^{n+1} states of the metal cations with NO. For all metal cations except scandium and manganese, these represent the ground and first excited states. Sc^+ and Mn^+ both have d^ns^1 ground states, $^3D(d^1s^1)$ and $^7S(d^5s^1)$, respectively, and d^ns^1 first excited states, $^1D(d^1s^1)$ and $^5S(d^5s^1)$. The second excited states of Sc^+ and Mn^+ are the lowest-lying d^{n+1} states, $^3F(d^2)$ and $^5D(d^6)$, respectively. For these two cases the reactivity of the three lowest states of the metal cations with NO is considered. For Ti^+, V^+, and Cr^+ we also considered $M(NO)^+$ states arising from low-spin d^{n+1} states of the metal cations. $M(NO)^+$ states arising from these excited states of the metal cations have the potential for greater covalent bonding contributions than those arising from the lower-lying d^ns^1 and d^{n+1} states. For Cu^+ we considered only the reactivity of the d^{n+1} ground state, $^1S(d^{10})$, as the d^ns^1 excited state is very high in energy.

4.1. Geometries. Table 1 shows the equilibrium geometries determined at the DFT level and the states' relative energies at the DFT level in the AW/DZP basis, at the CCSD(T) level in the AW/cc-pVTZ basis, and for the low-lying stationary states, at the CCSD(T) level in the AANO/cc-pVTZ basis set. Table 2 gives the vibrational frequencies calculated at the DFT level in the AW/DZP basis set. The orbital occupancies in the $M(NO)^+$ complexes are reported for the valence orbitals qualitatively described above and shown in Figure 1.

4.1.1. Sc(NO)$^+$, Ti(NO)$^+$, and V(NO)$^+$. $Sc(NO)^+$, $Ti(NO)^+$, and $V(NO)^+$ all have side-on geometries in their ground states. The ground-state geometry of $Sc(NO)^+$ is a $^2A''$ state with an orbital occupancy $1a'^2 1a''$. The ground state of $Ti(NO)^+$ is $^1A'$ with an orbital occupancy of $1a'^2 1a''^2$. Ground-state $V(NO)^+$ is $^2A'$. The orbital occupancy is $1a'^2 1a''^2 2a'$. The $Sc(NO)^+$ ground state arises from a mixture of $^3D(d^1s^1)$ and $^3F(d^2)$ states of Sc^+, see Table 3. Similarly, the ground states of $Ti(NO)^+$ and $V(NO)^+$ arise from a mixture of the d^ns^1 and d^{n+1} occupations of Ti^+ and V^+, but with low-spin couplings to produce molecular singlet and doublet states, respectively. The nearly equal M−N and M−O distances for all three complexes indicate that the metal is interacting equally with both atoms in the side-on NO. For both ground-state complexes the N−O bond distance is lengthened considerably from the free NO equilibrium bond distance at this same level of theory, 1.157 Å, and fall between the experimental bond distances for double and single N−O bonds of 1.25 Å and 1.41 Å. Weakening of the N−O bond can be seen in the lower vibrational frequencies of the N−O stretch in the early-metal complexes compared to free NO. The doubly occupied bonding orbital in the $^2A''$ state of $Sc(NO)^+$ is shown in Figure 2. The corresponding orbitals for $Ti(NO)^+$ and $V(NO)^+$ are very similar. It is composed of the in-plane 3d and NO π^* orbitals and clearly shows the metal orbital interacting with both nitrogen and oxygen.

4.1.2. Cr(NO)$^+$ to Ni(NO)$^+$. For ground states of $M(NO)^+$ (M = Cr-Ni), DFT predicts that the metal cation binds NO in a linear structure. These linear ground states arise primarily from the d^{n+1} states of the metal cations. Chromium, cobalt, and nickel cations have d^{n+1} ground occupations. Manganese and iron cations have d^{n+1} states as their second and first excited states, respectively. For all ground-state complexes the unpaired NO π^* electron is low-spin coupled with an unpaired electron in the lowest-lying d^{n+1} electronic configuration of the metal cations, forming a very weak covalent interaction.

The doubly occupied orbitals in the linear complexes are bonding orbitals composed of metal dπ and NO π^*, as shown in Figure 3 for the $^5\Pi$ state of $Cr(NO)^+$. The 1δ orbitals are occupied preferentially to the 1σ orbital because the 3dσ is destabilized relative to the other nonbonding orbitals by the presence of the NO. This destabilization is lessened by 4s3dσ hybridization which allows the dσ orbital to direct a portion of its electron density into the *xy*-plane, away from the interaction with the NO.

The M−N bond distances for the linear ground-state $M(NO)^+$ complexes vary from 1.639 Å for nickel to 1.908 Å for chromium. Unlike the M−N bonds, the N−O bonds vary by no more than 0.02 Å from the bond distance for free N−O, 1.157 Å, except in the case of $Ni(NO)^+$, where the N−O bond distance is 1.125 Å.

While none of the metal cations Cr^+-Ni^+ appear to bind NO in side-on geometries in their ground states, four of the six metals have excited-state geometries similar to those of ground-state $Sc(NO)^+$, $Ti(NO)^+$, and $V(NO)^+$. Excited states of $Cr(NO)^+$, $Mn(NO)^+$, and $Fe(NO)^+$ bind NO side-on and have elongated N−O distances and lower N−O stretching frequencies that indicate the N−O bond has been weakened. Compared to the ground states of the early-metal $M(NO)^+$ complexes, the middle- to late-metal complexes have longer M−N and M−O bonds and shorter N−O bond distances. This suggests that these excited states will not activate NO as effectively as the metals Sc^+-V^+.

4.1.3. Cu(NO)$^+$. Copper cation binds NO in a bent geometry in its $^2A'$ ground state. The complex is d^{10} in character and arises from the $^1S(d^{10})$ ground state of Cu^+. The orbital occupancy is $1a'(1\pi)^2 1a''(1\pi)^2 2a'(1\delta)^2 2a''(1\delta)^2 3a'(1\sigma)^2 4a'(2\pi)$. A plot of the singly occupied orbital in $Cu(NO)^+$ is shown in Figure 4. This orbital, $4a'(2\pi)$, is composed mainly of the Cu 4s and in-plane NO π^* orbitals and shows the bond formed between Cu^+ and NO. The Cu-N bond distance is 1.954 Å, the N−O bond distance is 1.142 Å, and the Cu−N−O angle is 132.94°. Donation of electronic density from the N−O π^* orbital to the Cu 4s shortens the N−O bond. This donation and contributions from the $^2D(d^9s^1)$ excited state of Cu^+ as well as the $^2S(d^{10}s^1)$ ground state of neutral Cu result in the formation of a one-electron Cu−N bond.

4.2. Energetics. Table 3 shows the metal 3d and 4s populations and the Mulliken charges on the metal centers for the ground-state complexes. Table 4 contains the binding energies for the ground-state and low-lying complexes. At the

TABLE 1: DFT Geometries for M(NO)$^+$ Expectation Values for S^2 at the DFT Level, and Relative Energies at the DFT and CCSD(T) Levels[a]

		geometry						relative energy			
metal	state[b]	r(M−N)	r(N−O)	r(M−O)	∠(M−N−O)	∠(N−M−O)	$\langle S^2\rangle$	DFT AW/DZP	CCSD(T) AW/cc-pVTZ	CCSD(T) AANO/cc-pVTZ	
Sc	^{2}A″	1.887	1.321	1.899	70.08	40.82	0.756	0.0	0.0	0.0	
	$^2\Pi$	1.833	1.194		180.0		0.778	10.65	7.6	13.02	
	^{2}A′	2.031	1.274	2.031	71.71	36.55	1.498	18.79	15.24		
	$^4\Delta$[c]	2.011	1.196		180.0				19.90		
	(^{4}A″)	2.089	1.249	2.101	73.19	34.68	3.758	19.29	21.37		
	^{4}A′	2.038	1.233	2.292	85.24	32.40	3.757	21.54	23.36		
	$^2\Sigma^+$	2.011	1.175		180.0		0.794	35.38	32.43		
Ti	^{1}A′	1.700	1.398	1.756	68.28	47.69	0.0	0.0	0.0	0.0	
	^{3}A″	1.829	1.287	1.899	90.31	40.32	2.009	3.94	14.67	16.10	
	$^3\Phi$	1.831	1.177		180.0		2.291	5.06	17.17	22.24	
	^{3}A′	1.834	1.261	2.002	78.19	38.06	2.020	6.68	20.65	20.34	
	$^5\Delta$	1.905	1.167		180.0		6.008	7.65	24.89	27.99	
	^{5}A′	2.069	1.233	2.096	73.96	34.43	6.007	18.93	32.19		
V	$^4\Pi$	1.865	1.15[d]		180.0		4.319	0.0	0.0	0.0	
	$^6\Sigma^+$	1.887	1.159		180.0		8.757	0.06	−6.31	3.23	
	^{4}A′	1.867	1.230	1.967	75.75	37.31	3.862	4.26		2.46	
	^{2}A′	1.757	1.312	1.839	71.97	42.71	1.491	8.96		−0.58	
	^{2}A″	1.780	1.284	1.890	74.22	40.82	1.393	10.66		1.68	
Cr	$^5\Pi$	1.908	1.151		180.0		6.716	0.0	0.0	0.0	
	^{7}A′	2.118	1.150		136.52		12.004	6.74	0.11	0.66	
	^{5}A′	1.998	1.190	2.075	76.60	33.90	6.375	6.87		4.11	
	($^7\Pi$)	2.086	1.152		180.0		12.003	9.51	1.95		
	^{7}A″	2.216	1.197	2.152	71.17	31.77	12.007	19.71	15.27	15.16	
	^{3}A″	1.813	1.273	1.890	73.17	40.15	3.033	27.81		34.95	
Mn	$^4\Sigma^-$	1.750	1.165		180.0		4.714	0.0	0.0	0.0	
	^{4}A″	1.826	1.232	2.040	81.17	36.62	4.807	14.54			
	^{6}A″	1.946	1.164		138.66		9.008	18.65	22.75		
	($^6\Sigma^+$)	1.877	1.169		180.0		8.995	23.35	22.06		
	^{8}A″	2.374	1.151		148.39		15.754	24.51	−1.49	1.95	
	($^6\Pi$)	2.138	1.147		180.0		8.758	44.54		39.29	
	($^4\Pi$)	1.796	1.165		180.0		3.803	63.71	74.59		
Fe	$^3\Delta$	1.722	1.158		180.0		2.748	0.0	0.0	0.0	
	$^3\Pi$	1.928	1.141		180.0		2.853	13.92	14.70	14.60	
	^{5}A″	1.852	1.153		146.75		6.067	14.40	17.77	19.90	
	($^5\Pi$)	1.828	1.158		180.0		6.053	16.77	17.90		
	^{5}A′	1.960	1.231	1.939	70.67	36.80	6.105	28.97	29.65		
	($^7\Delta$)	2.377	1.144		180.0		12.006	40.15	23.73		
	($^7\Pi$)	2.448	1.144		180.0		12.005	40.33	23.67		
Co	$^2\Sigma^+$	1.709	1.144		180.0		1.391	0.0	0.0	0.0	
	$^2\Delta$	1.691	1.142		180.0		1.358	0.12	−13.00	−0.40	
	^{4}A″	1.875	1.149		146.27		3.764	6.23	12.13	15.80	
	($^4\Phi$)	1.845	1.152		180.0		3.765	7.95	12.14		
	($^2\Pi$)	1.985	1.139		180.0		1.608	24.91	33.91		
	$^4\Delta$	1.885	1.118		180.0		4.219	41.96	31.63		
	^{6}A′	2.187	1.151		148.6		8.756	43.56			
	($^6\Pi$)	2.315	1.144		180.0		8.755	51.57			
Ni	$^1\Sigma^+$	1.639	1.125		180.0		0.0	0.0	0.0	0.0	
	^{3}A′	1.896	1.146		138.83		2.008	9.82	25.60	26.11	
	^{3}A″	1.911	1.145		133.80		2.006	10.63	26.54	27.58	
	($^3\Pi$)	1.863	1.147		180.0		2.010	14.40	27.97		
	($^3\Sigma^-$)	2.007	1.145		180.0		2.007	21.98	32.57		
	^{5}A″	2.105	1.152		147.41		6.006	55.39	62.01		
	($^5\Pi$)	2.262	1.143		180.0		6.004	55.97	62.59		
Cu	^{2}A′	1.954	1.142		132.94		0.756	0.0	0.0		
	($^2\Pi$)	1.897	1.145		180.0		0.753	3.90	1.77		

[a] Geometries in angstroms and degrees. Relative energies in kcal/mol. [b] States in parentheses have one or more imaginary frequencies. [c] Indicates the geometry was optimized manually at the CCSD(T) level. [d] Optimized manually at DFT level.

DFT level, energies uncorrected and corrected for state bias as described above are both reported. The CCSD(T) level energies are reported in both the AW/cc-pVTZ and AANO/cc-pVTZ basis sets. All dissociation energies are given with respect to the ground states of the atomic metal cations and ground-state NO, and are corrected for zero-point energy. The correction improves the agreement between the DFT and CCSD(T)/ AANO/cc-pVTZ binding energies for Sc, Mn, and Fe. For Ti, the correction significantly increases the disagreement, while for the remaining systems the correction increases the difference slightly. Perhaps the failure of the correction for Ti arises because the correction is determined for the highest spin states associated with the $d^n s^1$ and d^{n+1} occupations, whereas the bonding is derived from low-spin states associated with these occupations. Because the DFT values for both Ti and Ni are too small, it is also possible that DFT tends to underestimate the binding energies of singlet states. Since the corrected DFT binding energies are in slightly better agreement with the CCSD-(T)/ AANO/cc-pVTZ results, we use them for the rest of the discussion.

4.2.1. Ground States of V(NO)$^+$ through Co(NO)$^+$. In Table 1 for V(NO)$^+$ through Co(NO)$^+$ we see that there are small energetic spacings among the lowest lying states. For V(NO)$^+$, Mn(NO)$^+$, and Co(NO)$^+$ at the CCSD(T) level in the AW/cc-pVTZ basis set, there are states that are lower in energy than the state predicted by DFT to be the ground state. Such differences are consistent with the limitations of the B3LYP, especially in light of the poor S^2 values found for some states

TABLE 2: DFT Vibrational Frequencies for M(NO)$^+$ (M = Sc−Cu)

metal	state	vibrational frequencies (cm^{-1})			
Sc	^{2}A″	396.2	488.1	1158.2	
	$^2\Pi$	291.6	320.7	573.6	1635.7
	^{2}A′	323.4	391.1	1315.2	
	^{4}A″	516.3i	457.8	1561.5	
	$^4\Delta$	Not available: geometry optimized at CCSD(T) level			
	^{4}A′	253.5	495.6	1417.5	
	$^2\Sigma^+$	232.3	234.2	455.4	1795.4
Ti	^{1}A′	510.0	742.0	1107.8	
	^{3}A″	431.5	653.3	1253.9	
	$^3\Phi$	297.9	292.9	480.3	1734.2
	^{3}A′	451.5	585.8	1330.5	
	$^5\Delta$	217.9	217.9	501.9	1816.9
	^{5}A′	226.6	479.9	1476.6	
V	$^4\Pi$	187.3	211.8	418.2	1923.6
	$^6\Sigma^+$	197.1	197.1	487.4	1863.2
	^{4}A′	421.0	469.4	1470.8	
	^{2}A′	394.8	557.1	1197.0	
	^{2}A″	429.7	541.0	1267.8	
Cr	$^5\Pi$	183.4	231.1	360.5	1935.0
		(186.6	229.3	360.3	1950.5)[a]
	^{7}A′	198.2	309.4	1911.1	
	^{5}A′	288.4	396.0	1681.0	
	$^7\Pi$	227.4i	186.7	272.0	1938.5
	^{7}A″	148.3	266.5	1649.3	
	^{3}A″	422.0	490.0	1312.5	
Mn	$^4\Sigma^-$	265.2	265.3	531.1	1895.4
	^{4}A″	233.7	552.2	1463.7	
	^{6}A″	258.6	402.4	1767.6	
	$^6\Sigma^+$	329.7i	240.7	445.5	1828.0
	^{8}A″	75.3	245.8	1932.1	
	$^6\Pi$	197.3i	190.4	228.6	2001.3
	$^4\Pi$	200.6i	322.8	480.5	1876.7
Fe	$^3\Delta$	250.7	250.8	534.6	1948.3
	$^3\Pi$	68.9	205.3	303.3	2021.0
	^{5}A″	226.2	428.5	1894.8	
	$^5\Pi$	295.1i	276.0	436.3	1926.5
	^{5}A′	323.96	375.1	1476.1	
	$^7\Delta$	84.8i	114.0	152.0	2019.4
	$^7\Pi$	70.5i	98.1	159.6	2025.9
Co	$^2\Sigma^-$	186.5	236.8	433.7	1980.5
	$^2\Delta$	204.1	204.1	528.8	2009.1
	^{4}A″	159.9	368.3	1931.1	
	$^4\Phi$	230.3i	259.5	391.3	1973.9
	$^2\Pi$[b]	343.0i	95.0	506.7	1993.7
	$^4\Delta$	208.2	484.2	562.0	2090.2
	^{6}A′	70.7	277.6	1918.9	
	$^6\Pi$	90.2i	130.6	160.0	2025.0
Ni	$^1\Sigma^+$	226.8	226.8	619.0	2117.0
	^{3}A′	210.8	380.5	1949.5	
	^{3}A″	201.0	444.3	1962.6	
	$^3\Pi$	263.0i	210.4	363.4	2005.8
	$^3\Sigma^-$	258.7i	187.7	262.4	2027.4
	^{5}A″	127.9	305.9	1908.6	
	$^5\Pi$	103.0i	131.9	180.1	2032.6
Cu	^{2}A′	211.6	352.3	1985.9	
	$^2\Pi$	258.9i	213.0	328.7	2030.6
Free NO	$^2\Pi$	1950.0			
		(1971.5)[a]			

[a] Frequencies computed at the DFT level in the 6-311+G(2df) basis set. [b] Displacement along the imaginary mode results in collapse to the lowest doublet state.

of the systems with metal atoms from the middle of the row (see Table 1). CCSD(T) calculations in the AANO/cc-pVTZ basis help resolve uncertainties as to the ground states of these complexes. For Cr(NO)$^+$ and Fe(NO)$^+$ the order of the lowest-lying states is not altered by the use of the larger basis set in the CCSD(T) calculations. The ground-state predictions are consistent at all computational levels. For V(NO)$^+$, however, CCSD(T) calculations in the larger basis set predict the ^{2}A′ state to be the ground state, lying 0.58 kcal/mol below the $^4\Pi$ state.

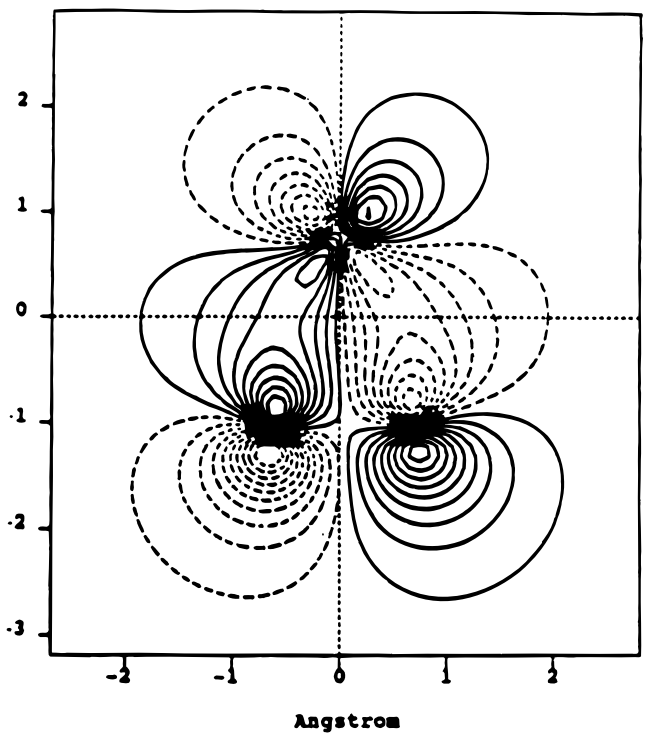

Figure 2. The σ-bonding orbital from DFT calculation of the ^{2}A″ state of Sc(NO)$^+$. The orbital plot shows overlap between the Sc 3d orbital and the NO π* orbital.

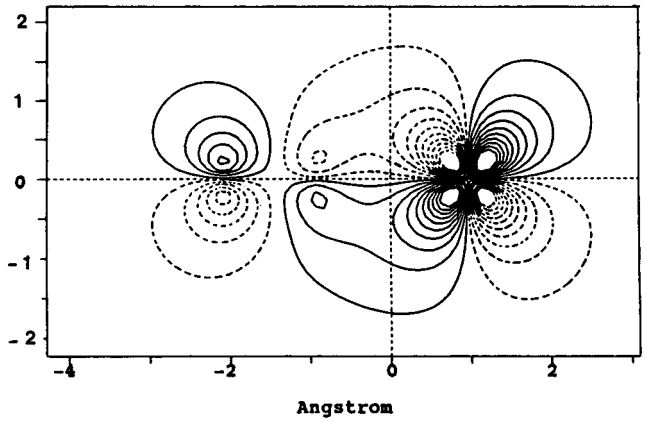

Figure 3. A π-bonding orbital from DFT calculation of the $^5\Pi$ state of Cr(NO)$^+$. The orbital plot shows overlap between a Cr dπ orbital and a NO π* orbital.

TABLE 3: Mulliken Populations of the 3d and 4s Orbitals in the Ground States of M(NO)$^+$

state	3d	4s	net charge on metal center
Sc(NO)$^+$ ^{2}A″	1.48	0.13	1.197
Ti(NO)$^+$ ^{1}A′	2.53	0.12	1.186
V(NO)$^+$ ^{2}A′	3.51	0.20	1.120
Cr(NO)$^+$ $^5\Pi$	4.76	0.24	0.888
Mn(NO)$^+$ $^4\Sigma^-$	5.62	0.21	1.000
Fe(NO)$^+$ $^3\Delta$	6.76	0.20	0.913
Co(NO)$^+$ $^2\Delta$	7.72	0.29	0.789
Ni(NO)$^+$ $^1\Sigma^+$	8.93	0.29	0.655
Cu(NO)$^+$ ^{2}A′	9.88	0.30	0.728

The ^{2}A″ and ^{4}A′ states lie between the $^4\Pi$ and $^6\Sigma^+$ states at the CCSD(T) level in the larger basis set. This is in contrast the DFT results which place the bent doublet and quartet states above the $^6\Sigma^+$ state in energy. The Mn(NO)$^+$ ground state calculated with CCSD(T) in the larger basis set agrees with the DFT result of $^4\Sigma^-$ though the ^{8}A″ state lies much closer in energy to the ground state at the CCSD(T) level in the AANO/cc-pVTZ basis set than at the DFT level. For Co(NO)$^+$,

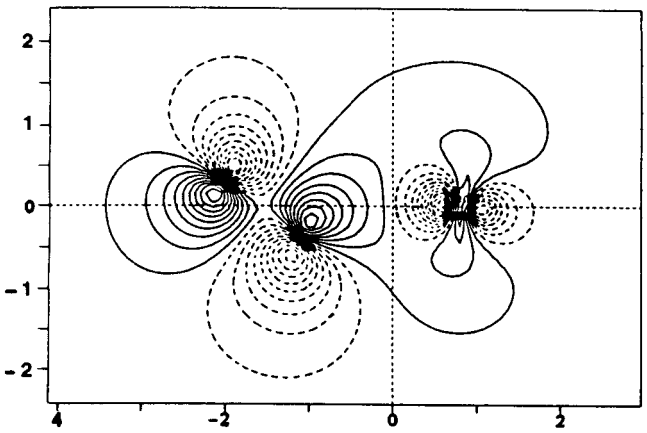

Figure 4. The singly occupied bonding orbital from DFT calculation of the $^2A'$ state of $Cu(NO)^+$. The orbital plot shows overlap between the in-plane Cu 3d orbital with significant contributions from the 4s and the NO in-plane π^* orbital.

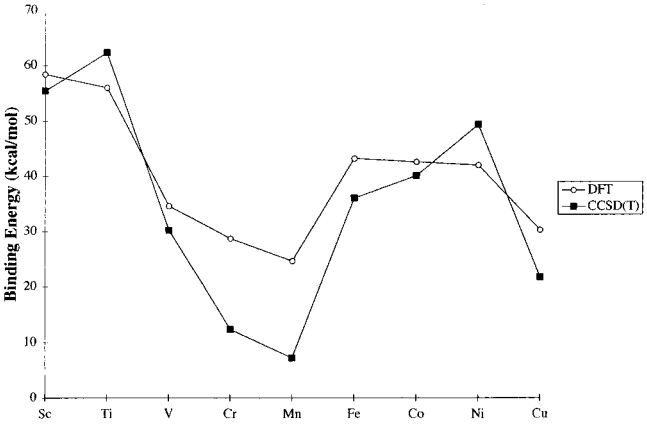

Figure 5. Plot of DFT and CCSD(T) binding energies. The plot shows the trends in the binding energies at the DFT level corrected for state bias and at the CCSD(T) level in the AANO/cc-pVTZ basis set. Both DFT and CCSD(T) values are corrected for zero-point energy as described in the text.

TABLE 4: DFT and CCSD(T) Binding Energies for Ground State $M(NO)^+$ [a]

State	D_0 (DFT) AW/DZP	D_0 (DFT) (corr[b]) AW/DZP	D_0[CCSD(T)] AW/cc-pVTZ	D_0[CCSD(T)] AANO/ cc-pVTZ
$Sc(NO)^+$ $^2A''$	62.76	58.42	45.26	55.46
$Ti(NO)^+$ $^1A'$	60.03	56.07	53.91	62.39
$V(NO)^+$ $^2A'$	32.49	34.60		30.19
$Cr(NO)^+$ $^5\Pi$	28.03	28.67	10.81	12.33
$Mn(NO)^+$ $^4\Sigma^-$	32.78	24.64	2.78	7.18
$Fe(NO)^+$ $^3\Delta$	50.15	43.13	31.40	35.96
$Co(NO)^+$ $^2\Delta$	40.90	42.51	39.01	40.02
$Ni(NO)^+$ $^1\Sigma^+$	41.76	41.87	46.75	49.26
$Cu(NO)^+$ $^2A'$	30.00	30.20	19.81	21.68

[a] In kcal/mol. [b] corr = corrected.

however, the CCSD(T) calculations in the two basis sets agree, both in disagreement with the ground state predicted by DFT. In this case we believe the CCSD(T) calculations are correct, and the ground state of $Co(NO)^+$ is $^2\Delta$.

4.2.2. Trends. The trends in the binding energies across the row are shown in Figure 5 where the corrected DFT binding energies and CCSD(T) binding energies calculated in the AANO/cc-pVTZ basis set are plotted. For scandium and titanium, the CCSD(T) values shown in Figure 5 are those calculated in the AANO3s3p/cc-pVTZ basis set. The CCSD(T) energies shown for $V(NO)^+$, $Mn(NO)^+$, and $Co(NO)^+$ are those binding energies for the $^2A'$, $^4\Sigma^-$, and $^2\Delta$ states, respectively.

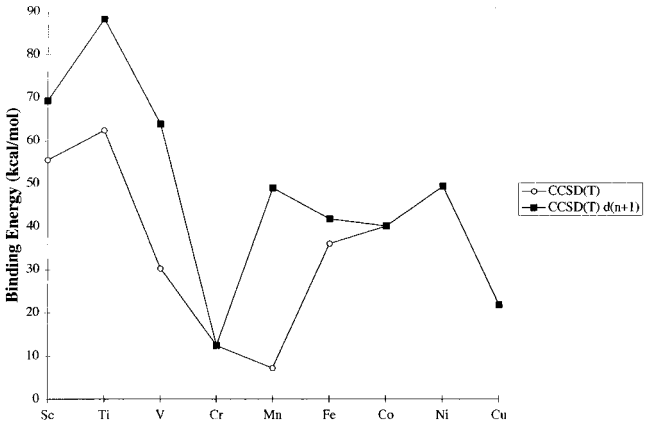

Figure 6. Plot of the CCSD(T) binding energies versus the ground states and the lowest-lying d^{n+1} states of the metal cations. Binding energies were calculated in the AANO/cc-pVTZ basis set and corrected for zero-point energy. The energies of the d^{n+1} states for Sc^+, Ti^+, Mn^+, and Fe^+ were obtained by adding the experimental value for the ground-state/d^{n+1} separation energy.

At the DFT level, the most strongly bound complex in the first transition row is $Sc(NO)^+$. CCSD(T) results, however, show the largest binding energy for $Ti(NO)^+$. For $Sc(NO)^+$, the DFT binding energy is 3.0 kcal/mol larger than the CCSD(T) binding energy, while for $Ti(NO)^+$ the DFT binding energy is 6.4 kcal/mol smaller than the CCSD(T) value.

The metals in the middle of the periodic table exhibit an even larger disparity between the DFT and CCSD(T) binding energies, with DFT results being significantly larger than the CCSD(T) values. Both methods yield a small binding energy for $Cr(NO)^+$, where the large Cr^+ exchange energy results in minimal covalent bonding in $Cr(NO)^+$. The difference between DFT and CCSD(T) binding energies for $Cr(NO)^+$ and $Mn(NO)^+$ is ~17 kcal/mol. The difference between DFT and CCSD(T) binding energies decreases for $Fe(NO)^+$ and $Co(NO)^+$ at 7.1 and 1.5 kcal/mol. The $^1\Sigma^+$ ground state of $Ni(NO)^+$ shows behavior similar to $Ti(NO)^+$, in that the DFT binding energy is smaller than the CCSD(T) binding energy by 7.4 kcal/mol.[44] Ground-state $Cu(NO)^+$ binding energies at the DFT and CCSD(T) levels show behavior consistent with that of the other $M(NO)^+$ complexes. The DFT binding energy is 9.8 kcal/mol larger than the CCSD(T) binding energy.

To establish whether a larger basis set for the DFT calculations would decrease the discrepancy between the DFT and CCSD(T) binding energies in these complexes we calculated the geometry and binding energy of $Cr(NO)^+$ in the larger DFT basis set. In the 6-311+G(2df) basis, the geometry does not change significantly and the binding energy, 26.67 kcal/mol, is less than three kcal/mol smaller than the DFT results for the binding energy in the AW/DZP basis set, 29.12 kcal/mol.

It is also interesting to compare the CCSD(T) binding energies with respect to the ground states with those calculated with respect to the lowest-lying d^{n+1} states of the metal cations from which the complex could have formed. These are shown in Figure 6. The values used for the excitation energies of the cations Sc^+, Ti^+, V^+, Mn^+, and Fe^+ were the experimental values.[45] Most notable is that the binding energies of $Ti(NO)^+$, $V(NO)^+$, and $Mn(NO)^+$ are now significantly larger. This is because $^1A'$ $Ti(NO)^+$, $^2A'$ $V(NO)^+$, and $^4\Sigma^-$ $Mn(NO)^+$ arise from higher-lying excited states of the metal cations. The low binding energy of $Cr(NO)^+$ can be explained by high exchange energy of Cr^+ that would resist pairing an electron in the half-filled d-shell with the electron in the π^* orbital of NO.

5. Discussion

From our results, we see that transition metal cations bind NO in several different ways. Scandium, titanium, and vanadium form ground-state complexes that contain partially activated N−O bonds. Other first-row metals, however, appear to have the capability to partially activate the N−O bond only in their excited states. The bonding in ground states of the early metals is different from the rest of the first row in that the metal center is bonding with both atoms in NO. A natural bond orbital analysis[46] (NBO) of the DFT orbitals for $Sc(NO)^+$ reveals that the bonding orbitals are two Sc−N bonds, one in-plane, one out-of-plane, and one Sc−O bond. The in-plane Sc−N orbital is 27% Sc 3d/77% N 2p and doubly occupied. The out-of-plane, singly occupied Sc−N bonding orbital is 23% Sc 3d/77% N 2p. The doubly occupied, in-plane Sc−O bonding orbital is composed of 13% Sc 3d/87% O 2p. The Mulliken charge on the metal center also differentiates $Sc(NO)^+$, $Ti(NO)^+$, and $V(NO)^+$ from the other $M(NO)^+$ complexes, see Table 3. All three metals, Sc−V have charges greater than 1, indicating that both complexes have contributions from $M^{2+} + NO^-$.

In the linear ground states of $M(NO)^+$ for chromium through nickel, where the metal cations do not attack the N−O bond, the N−O bond distances are only slightly perturbed from the free N−O distance. Bonding in these complexes could arise from several sources: charge-dipole interaction between the metal cation and NO, covalent interaction between the partially filled NO π^* orbital and partially filled metal orbitals, and dative bonding between filled metal orbitals to the other, empty NO π^* orbital as well as between the NO lone pair and an empty metal orbital. We can see from the charges in the metal atoms shown in Table 3 that the $M(NO)^+$ complexes in the middle of the row show very little net charge transfer. An NBO analysis for $Cr(NO)^+$ reveals that this complex and, by analogy, most of the other linear ground states, undergo a combination of electrostatic bonding and dative bonding. The analysis shows no metal−ligand bonding orbitals but does indicate donation from the nitrogen lone pair orbital to the empty 4s orbital on Cr and backdonation from the singly occupied dπ orbitals to the NO π^* orbitals.

Toward the end of the first transition row we begin to see more substantial contributions from $M^0 + NO^+$. $Ni(NO)^+$ has a shorter N−O bond distance, 1.125 Å, relative to the other middle-to-late metal complexes. This short N−O distance, as well as the shorter metal−N bond distance for $Ni(NO)^+$, arises from the strong charge transfer contribution to the bonding in this complex. For $Ni(NO)^+$ the Mulliken charge on the Ni center is +0.66, indicating that there is a large contribution to the bonding from Ni^0 and NO^+. The equilibrium bond distance for free NO^+ is 1.067 Å at the DFT level, and allowing for a 34% contribution from the charge transfer products, a bond distance of approximately 1.127 Å would be expected for $Ni(NO)^+$.

By looking at how DFT and CCSD(T) treat the ionization potentials (IP) of Ni and NO, compared to experiment, we can evaluate how effective each method would be at treating contributions to the bonding from $Ni + NO^+$. The Ni IP of interest is the energy difference between the $^3D(d^9s^1)$ first excited state of Ni and $^2D(d^9)$ ground state of Ni^+. The experimental value is 7.55 eV.[45] The DFT value is too large, 7.93 eV, while the CCSD(T) value is too small, 7.11 eV. The NO IP at the DFT and CCSD(T) levels are given in the Methods section above. The Δ(IP) for Ni and NO at the experimental level is, therefore, 1.55 eV. At the DFT level this value is 1.78 eV, and the CCSD(T) value is 1.76 eV. This disagreement with experiment indicates that neither the DFT nor the CCSD(T) description of the bonding for $Ni(NO)^+$ contains a large enough contribution from $Ni^0 + NO^+$.

$Cu(NO)^+$ is the only ground-state complex of the first row transition metals that could have an electron in one of the high-energy antibonding orbitals. The complex avoids this unfavorable interaction by forming a bent structure and localizing the Cu^+ and NO π^* orbitals. Bending also introduces a dative contribution to the bonding in $Cu(NO)^+$. An NBO analysis of the orbitals in $^2A'$ $Cu(NO)^+$ shows that there is a one-electron bond formed between the Cu center and the nitrogen of NO. The singly occupied orbital is 12% Cu and 88% N. The copper orbital is 93% 4s, 3% 4p, and 4% 3d; the nitrogen orbital is 9% 2s and 91% 2p. The low metal charge seen in the ground state of $Cu(NO)^+$ is indicative of electron density being donated to the metal center to form the bond with the NO.

The geometry reported by Hrušák et al. for the ground state of $Cu(NO)^+$, obtained at the CCSD(T) level in their first basis set, BS1, has a Cu−N bond distance of 2.045 Å, an N−O distance of 1.201 Å, and a bond angle of 157.3°. These are different from our DFT geometry results, especially in that our N−O bond distance is shorter than the N−O distance for free NO, while the value reported by Hrušák et al. is longer. To resolve this disagreement, we optimized the geometry of $Cu(NO)^+$ at the CCSD(T) level using the AANO/cc-pVTZ basis set. The results of this geometry optimization agree with the structure predicted by DFT. The Cu-N distance, 1.984 Å, is 0.03 Å longer than that of our DFT geometry. The N−O distance is 1.144 Å, which agrees with the DFT value, as does the Cu-N−O bond angle, 135.9°. The total energy of the structure optimized at the CCSD(T) level was 0.28 kcal/mol lower than the CCSD(T) total energy calculated for the DFT structure. The CCSD(T) prediction of a N−O bond distance in $Cu(NO)^+$ shorter than free NO supports our analysis that the NO donates electron density to Cu^+ for the bonding in $Cu(NO)^+$. The agreement between the DFT and CCSD(T) geometries justifies our decision to use DFT for determining the structures of the $M(NO)^+$ complexes. The difference between our CCSD(T) results and those of Hrušák et al. results from the lack of polarization functions in their basis set denoted BS1.

The energetic results closest in methodology to our own are the results for the CCSD(T) calculations performed in their largest basis set, BS4. At this level Hrušák et al. report the bond dissociation energy of $Cu(NO)^+$ $^2A'$ as 19.7 kcal/mol. This is in agreement with our CCSD(T) calculated value of 21.68 kcal/mol. They estimate a value corrected for basis set incompleteness and remaining correlation energy as 28 ± 8 kcal/mol.

Both our work and that of Hrušák et al. disagree with that published by Benjelloun et al. Our results show that the $^2A'$ state at the DFT level lies 3.90 kcal/mol below the $^2\Pi$ state predicted in the work of Benjelloun et al. to be the ground state. Their lowest-lying $^2A'$ state is the first excited state, 19.83 kcal/mol above their $^2\Pi$ state, and it is shown to be an intermediate on the reaction pathway that converts $Cu(NO)^+$ to $Cu(ON)^+$. Hrušák et al. do not report results for the $^2\Pi$ state, but do report the ground state as $^2A'$. Our DFT harmonic frequencies show that the $^2\Pi$ state is a transition state between the bent structures for ground-state $Cu(NO)^+$.

Benjelloun et al. suggest that the difference between their geometry and that of Hrušák et al. could be due to the UHF reference used by Hrušák et al. This does not appear to be the case since our CCSD(T) is based on an RHF approach. In order to better understand the origin of the difference in the $CuNO^+$ results, we performed singles and doubles CI (SDCI) and CCSD(T) calculations using the AW/cc-pVTZ basis set at the B3LYP

optimal linear and bent geometries. The SDCI places the bent structure 1.96 kcal/mol below the linear structure, which is in excellent agreement with the CCSD and CCSD(T) results for the difference between the structures of 1.93 and 1.91 kcal/mol, respectively. These are also in reasonable agreement with the B3LYP value of 3.9 kcal/mol. The most important (mass−velocity and Darwin) relativistic effects can be computed at the SDCI level using first order perturbation theory. These stabilize the bent structure by 0.11 kcal/mol relative to the linear. This is consistent with the larger NO donation to the Cu 4s orbital for the bent structure. We therefore conclude that $CuNO^+$ is bent. We speculate that the results of Benjelloun et al. could be due to their smaller basis set, their use of an effective core potential, or their configuration selection procedure.

6. Conclusions

We have shown that, while the $M(NO)^+$ complexes of the first-transition-row elements, M = Sc−Cu are challenging to treat, they are by no means impossible. The values calculated for the $M(NO)^+$ binding energies in this study agree very well both with experimental and other theoretical values. For $Fe(NO)^+$, our CCSD(T) value of 35.96 kcal/mol falls within the range proposed by Cassady and Freiser: $34 \pm 2 < D_0(Fe(NO)^+) < 58 \pm 2$ kcal/mol; as does our $Co(NO)^+$ value of 40.02 kcal/mol, $37 \pm 2 < D_0(Co(NO)^+) < 52 \pm 2$ kcal/mol. Results for both metals fall closer to the lower end of the range. Our value for the binding energy of $Ni(NO)^+$, 49.26 kcal/mol, is in good agreement with the value reported by Khan et al., $D_0(Ni(NO)^+) = 54 \pm 2$ kcal/mol. For $V(NO)^+$, $Mn(NO)^+$, and $Co(NO)^+$ where there are two or more states very close in energy to the ground state, DFT results and CCSD(T) results in the AANO/cc-pVTZ basis set predict the same ground state for $Mn(NO)^+$, but disagree for $V(NO)^+$ and $Co(NO)^+$. DFT overbinds the ground states of the $M(NO)^+$ complexes, except for $Ti(NO)^+$ and $Ni(NO)^+$, which it underbinds. We feel that our best binding energies CCSD(T) binding energies calculated in a large basis set.

Acknowledgment. Two of the authors (M.B.H. and J.L.C.T.) would like to thank the National Science Foundation (Grant CHE 94-13634) for financial support. J.L.C.T. would like to thank Dennis Marynick for helpful discussions and the National Aeronautics and Space Administration for financial support (Grant NGT-51337). This research was conducted in part with use of the Cornell Theory Center, a resource for the Center for Theory and Simulation in Science and Engineering at Cornell University, which is funded in part by the National Science Foundation, New York State, and IBM Corp.

References and Notes

(1) Wink, D. A.; Grisham, M. B.; Mitchell, J. B.; Ford, P. C. *Methods in Enzymology, Vol. 268*, Packer, L., Ed.; Academic Press: San Diego, 1996; p.12.

(2) Rutherford, J. A.; Mathis, R. F.; Turner, B. R.; Vroom, D. A. *J. Chem. Phys.* **1971**, *55*, 3785. Rutherford, J. A.; Mathis, R. F.; Turner, B. R.; Vroom, D. A. *J. Chem. Phys.* **1972**, 56, 4654. Rutherford, J. A.; Mathis, R. F.; Turner, B. R.; Vroom, D. A. *J. Chem. Phys.* **1972**, *57*, 3087. Rutherford, J. A.; Vroom, D. A. *J. Chem. Phys.* **1972**, *57*, 3091.

(3) Cadel, R. D. *Particles in the Atmosphere and Space*, Reinhold: New York, 1966.

(4) Schlögl, R. *Angew. Chem.* **1993**, *105*, 402.

(5) Freiser, B. S., Ed. *Organometallic Ion Chemistry*; Kluwer: Dordrecht, 1996. Russell, D. H., Ed. *Gas Phase Inorganic Chemistry*; Plenum: New York, 1990.

(6) Cassady, J. C.; Freiser, B. S. *J. Am. Chem. Soc.* **1985**, *107*, 1566.

(7) Khan, F. A.; Steele, D. L.; Armentrout, P. B. *J. Phys. Chem.* **1995**, *99*, 7819.

(8) Sülzle, D.; Schwarz, H.; Moock, K. H.; Terlouw, J. K. *Int. J. Mass Spectrom. Ion. Processes* **1991**, *108*, 269.

(9) Oriedo, J. V. B.; Russell, D. H. *J. Am. Chem. Soc.* **1993**, *115*, 8381.

(10) (a) Niuwenhuys, B. E. *Surf. Sci.* **1989**, *219*, 467. (b) Basch, H. *Chem. Phys. Lett.* **1985**, *116*, 58.

(11) Hrušák, J.; Koch, W.; Schwarz, H. *J. Chem. Phys.* **1994**, *101*, 3898.

(12) Benjelloun, A. T.; Daoudi, A.; Berthier, G.; Rolando, C. *THEOCHEM* **1996**, *360*, 127.

(13) Bauschlicher, C. W.; Bagus, P. S. *J. Chem. Phys.* **1984**, *80*, 944.

(14) Carter, E. A.; Smith, G. W. *J. Phys. Chem.* **1991**, *95*, 2327.

(15) Bauschlicher, C. W.; Ricca, A.; Partridge, H.; Langhoff, S. R. *Recent Advances in Density Functional Methods, Part II*; Chong, D. P., Ed.; World Scientific: Singapore, 1997.

(16) Wachters, A. J. H. *J. Chem. Phys.* **1970**, *52*, 1033.

(17) Hay, P.J. *J. Chem. Phys.* **1977**, *66*, 4377.

(18) Bauschlicher, C. W. *Theor. Chim. Acta* **1995**, *92*, 183.

(19) Raghavachari, K.; Trucks, G. W. *J. Chem. Phys.* **1989**, *91*, 1062.

(20) Frisch, M. J.; Pople, J. A.; Binkley, J. S. *J. Chem. Phys.* **1984**, *80*, 3265.

(21) Partridge, H. *J. Chem. Phys.* **1989**, *90*, 1043.

(22) (a) Almlöf, J.; Taylor, P. R. *J. Chem. Phys.* **1987**, *86*, 4070. (b) Bauschlicher, C. W.; Taylor, P.R. *Theor. Chim. Acta* **1993**, *86*, 13.

(23) van Duijneveldt, F. B. *IBM Research Report RJ 495;* 1971.

(24) Exponent for nitrogen is 0.75. Exponent for oxygen is 0.85.

(25) (a) Dunning, T. H. *J. Chem. Phys.* **1989**, *90*, 1007. (b) Woon, D. E.; Dunning, T. H. *J. Chem. Phys.* **1993**, *98*, 1358.

(26) Krishnan, R.; Binkley, J. S.; Seeger, R.; Pople, J. A. *J. Chem. Phys.* **1980**, *72*, 650.

(27) (a) Ditchfield, R.; Hehre, W. J.; Pople, J. A. *J. Chem. Phys.* **1971**, *54*, 724. (b) Hehre, W. J.; Ditchfield, R.; Pople, J. A. *J. Chem. Phys.* **1972**, *56*, 2257. (c) Hariharan, P. C.; Pople, J. A. *Mol. Phys.* **1974**, *27*, 209. (d) Gordon, M. S. *Chem. Phys. Lett.* **1980**, *76*, 163. (e) Harharan, P. C.; Pople, J. A. *Theor. Chim. Acta* **1973**, *28*, 213.

(28) Becke, A. D. *J. Chem. Phys.* **1993**, *98*, 5648 and references therein.

(29) Becke, A. D. *Phys. Rev.* **1988**, *A38*, 3098.

(30) Lee, C.; Yang, W.; Parr, R. G. *Phys. Rev.* **1988**, *B37*, 785.

(31) Vosko, S. H.; Wilk, L.; Nusair, M. *Can. J. Chem.* **1980**, *58*, 1200.

(32) Stephens, P. J.; Devlin, F. J. ; Chablowski, C. F.; Frisch, M. J. *J. Phys. Chem.* **1994**, *98*, 11623.

(33) (a) Barlett, R. J. *Annu. Rev. Phys. Chem.* **1981**, *32*, 359. (b) Pople, J. A.; Krishnan, R.; Schlegel, H. B.; Binkley, J. S. *Int. J. Quantum Chem.* **1978**, *14*, 545. (c) Cisek, J. *Adv. Chem. Phys.* **1969**, *14*, 35. (d) Purvis, G. D.; Barlett, R. J. *J. Chem. Phys.* **1982**, *76*, 1910. (e) Scuseria, G. E.; Janssen, C. L.; Schaefer, H. F. *J. Chem. Phys.* **1989**, *90*, 3700. (f) Handy, N. C.; Pople, J. A.; Head-Gordon, M.; Raghavachari, K.; Trucks, G. W. *Chem. Phys. Lett.* **1989**, *164*, 185.

(34) (a) Raghavachari, K.; Trucks, G. W.; Pople, J. A.; Head-Gordon, M. *Chem. Phys. Lett.* **1989**, *157*, 479. (b) Pople, J. A.; Head-Gordon, M.; Raghavachari, K. *J. Chem. Phys.* **1987**, *87*, 5968. (c) Watts, J. D.; Gauss, J.; Barlett, R. J. *J. Chem. Phys.* **1993**, *98*, 8718.

(35) (a) Hampel, C.; Peterson, K.; Werner, H.-J. *Chem.Phys. Lett.* **1992**, *190*, 1. (b) Hampel, C.; Peterson, K.; Werner, H.-J. *J. Chem. Phys.* **1993**, *99*, 5219.

(36) Ricca, A.; Bauschlicher, C. W. *Chem. Phys. Lett*. **1995**, *245*, 150.

(37) Huber, K. P.; Herzberg, G. *Molecular Spectra and Molecular Structure Constants of Diatomic Molecules*; Van Nostrand: New York, 1979.

(38) Clement, M. J. Y.; Ramsay, D. A. *Can. J. Phys*. **1961**, *39*, 205.

(39) Barnes, L. A.; Bauschlicher, C. W. *J. Chem. Phys.* **1989**, *91*, 314.

(40) Frisch, M. J.; Trucks, G. W.; Schlegel, H. B.; Gill, P. M. W.; Johnson, B. G.; Robb, M. A.; Cheeseman, J. R.; Keith, T. A.; Petersson, G. A.; Montgomery, J. A.; Raghavachari, K.; Al-Laham, M. A.; Zakrzewski, V. G.; Ortiz, J. V.; Foresman, J. B.; Cioslowski, J.; Stefanov, B. B.; Nanayakkara, A.; Challacombe, M.; Peng, C. Y.; Ayala, P. Y.; Chen, W.; Wong, M. W.; Andres, J. L.; Replogle, E. S.; Gomperts, R.; Martin, R. L.; Fox, D. J.; Binkley, J. S.; Defrees, D. J.; Baker, J.; Stewart, J. P.; Head-Gordon, M.; Gonzales, C.; Pople, J. A. GAUSSIAN94 Gaussian, Inc.: Pittsburgh, PA, 1995.

(41) MOLPRO is a package of *ab initio* programs written by H.-J. Werner and P. J. Knowles, with contributions from J. Almlof, R. D. Amos, M. J. O. Deegan, S. T. Elbert, C. Hampel, W. Meyer, K. Peterson, R. Pitzer, A. J. Stone, P. R. Taylor, and R. Lindh.

(42) (a) Hoffmann, R. J. *Chem. Phys.* **1963**, *39*, 1397. (b) Alvarez, S. *Table of Parameters for Extended Hückel Calculations*; Universitat de Barcelona, June 1989; CAChe Scientific (Release 3.5), Inc. copyright 1993.

(43) (a) Clemmer, D. E.; Aristov, N.; Armentrout, P. B. *J. Phys. Chem.* **1993**, *97*, 544; (b) Clemmer, D. E.; Elkind, J. L.; Aristov, N.; Armentrout, P. B. *J. Chem. Phys.* **1991**, *95*, 3387; (c) Aristov, N.; Armentrout, P. B. *J. Chem. Phys.* **1986**, *90*, 5135.

(44) $Ti(NO)^+$ and $Ni(NO)^+$ were also studied using spin-unrestricted DFT, but in each case the spin restricted solution was found to be the lowest.

(45) Moore, C. E. *Atomic Energy Levels As Derived from the Analysis of Optical Spectra; Circular 467*; National Bureau of Standards, Department of Commerce: Washington, DC, 1971; Vols. I and II.

(46) Reed, A. E.; Curtiss, L. A.; Weinhold, F. *Chem . Rev.* **1988**, *88*, 899 and references therein.